UC Irvine
UC Irvine Previously Published Works

Title
Plasma heating with a rotating relativistic electron beam. I. Return current processes

Permalink
https://escholarship.org/uc/item/4ck6c7bb

Journal
Physics of Fluids, 20(3)

ISSN
00319171

Authors
Molvig, Kim
Rostoker, Norman

Publication Date
1977

DOI
10.1063/1.861888

Peer reviewed

eScholarship.org Powered by the California Digital Library
University of California

Plasma heating with a rotating relativistic electron beam. I. Return current processes

Kim Molvig

Physics Department, University of California, Irvine, California 92664
and Research Laboratory of Electronics, Massachusetts Institute of Technology, Cambridge, Massachusetts 02139

Norman Rostoker

Physics Department, University of California, Irvine, California 92664
(Received 29 December 1975; final manuscript received 16 November 1976)

An advantageous configuration for plasma heating with a relativistic beam utilizes an annular beam rotating about a guide magnetic field. The return current processes for such a configuration are considered. For the parameters expected to prevail in an experiment, the plasma response can be described as magnetic diffusion or critically damped magnetosonic waves, these being equivalent. Equations for the axial and angular return currents are derived and take the form of decoupled diffusion equations. The effects of pulse shape, boundary conditions, etc. are then treated. The drag force on the beam resulting from the interaction is greatly enhanced and leads to a stopping length reduction by the factor $(1/2)(v_\parallel/c)^3$ as compared with nonrotating beams. The implications of these effects for a plasma heating application are discussed.

I. INTRODUCTION

It has been recognized for some time[1] that intense relativistic electron beams provide an attractive energy source for plasma heating. Previously studied processes[2] for coupling the beam energy into the plasma have concentrated on the linear configuration where the beam is simply injected along a guiding magnetic field. Enhanced coupling then results from the development of instabilities; either the two-stream instability between the primary beam electrons and plasma electrons, or the ion acoustic instability associated with the back-streaming plasma electrons of the return current.[3] Here, we consider the beam-plasma interaction for a configuration in which an annular rotating electron beam[4] is injected into a plasma. Particular interest attaches to the case when the ratio of rotational to parallel velocities $(v_\perp/v_\parallel)$ is high. This configuration has three principal advantages:

(i) The anomalous stopping power (inverse stopping length) of the plasma to the beam is enhanced over that for a nonrotating beam by the factor $2(c/v_\parallel)^3$. This factor can, in practical situations, be made quite large.

(ii) Beam energy can be coupled directly to the ions by the cross-field current.

(iii) Coupling mechanisms are classical and complete; the theoretical coupling efficiency is 100%.

To be more specific, we refer to the experimental situation as depicted in Fig. 1 and represented by the parameters of Table I. The envisioned sequence of events is as follows. Upon leaving the cusped magnetic field (which produces the beam rotation), the beam induces counter currents in the plasma. Concomitant fields brake the beam, trapping it in the magnetic mirrors, maintaining the rotation. Beam electrons lose a small fraction $\Delta E = \frac{1}{2}\gamma m v_\parallel^2 \ll (\gamma - 1)mc^2$ of their kinetic energy during this stage of the interaction. The trapping takes a fraction of an ion gyro period. Thus, in a time negligible with respect to the ions, a theta current is turned on within the plasma. Magnetosonic shock-type wave emissions follow and carry off the remaining beam energy. Since the wave energy is half magnetic and half ion particle energy, multi-kilovolt ion energies should be obtainable in a dense plasma even with a relatively modest electron beam.

The magnetosonic wave emission and ion heating are discussed in the second paper (II). The present paper deals with the return current processes for a rotating beam.

This problem was first considered by Chu and Rostoker,[5] who pointed out that the azimuthal beam current could be neutralized by an $\mathbf{E} \times \mathbf{B}$ drift of the plasma electrons. The theory of Chu and Rostoker considers a specific beam model and is not readily extended to include realistic beam profiles, current rise times, boundary conditions, etc. In addition, the theory relies on a specific (Langevin) form of the friction term in the fluid equations, and it is by no means clear that other forms (i.e., classical) give the same results. The purpose of this paper is to give a treatment which is both simpler and more general than that of Ref. 5. Specifically, the case Chu and Rostoker considered can

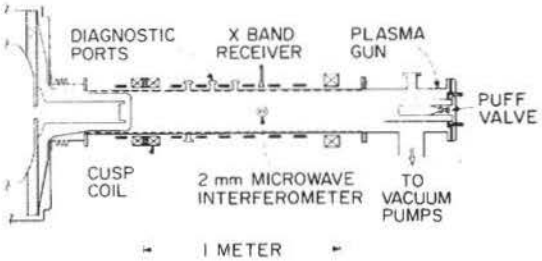

FIG. 1. Configuration for the plasma heating experiment.

Copyright © 1977 American Institute of Physics

TABLE I. Experimental parameters for a typical small scale plasma heating experiment.

Beam density	$n_b \sim 10^{11}$ cm^{-3}
Parallel velocity	$v_\parallel \sim 3\times10^9$ cm/sec
Perpendicular velocity	$v_\perp \sim c$
Beam radius	$r_0 \sim 5$ cm
Beam thickness	$a \sim 1$ cm
Guide field	$B_0 \sim 1$ kG
Plasma density	$n_p \sim 10^{14}$ cm^{-3}
Collision frequencies	$\nu_i \sim \nu_e \sim 10^9$ sec^{-1}

be reduced, *without any additional assumptions* to a pair of decoupled diffusion equations for the axial and angular return currents. In this form, the theory can easily be applied to a variety of practical situations. We also find that the classical form for the friction gives nearly the same results at sufficiently high collision frequencies. There is one noteworthy difference, however. In the limit where the results compare, there is a separate, additive ion contribution to the interaction (this was emphasized in Ref. 5) arising from the Langevin dissipation that does *not* appear when a classical friction term is used. For this reason, we are inclined to de-emphasize this ion term. It is nearly negligible for the experimental parameters listed in Table I.

Section II gives a discussion of the plasma response in physical terms, narrowing the scope somewhat for the following calculations. In Sec. III, we derive equations describing the angular and axial return current processes. Some consequences of the solutions, such as the disposition of beam energy, the modifications made by a finite beam rise time, and conducting wall effects are considered in Sec. IV. Finally in Sec. V, we calculate the anomalous stopping power, beam energy loss, and summarize the features and scaling laws of most importance for the plasma heating application.

II. PLASMA RESPONSE

Throughout this paper we will use a test particle model, where the beam is regarded as a specified current source to drive a plasma response. The beam is immersed in the plasma and the interaction turned on at $t = 0$. Such a model neglects the details of the diode region (and cusped field region for the rotating beam) and the initial entrance of the beam into the plasma. Transients of the model are therefore not realistic, and we consider only the steady response. For relativistic beams there is an added justification for doing this, since the beam will quickly outrun the transients, which propagate at group velocities much less than c.

When a coupling exists, the beam will excite all modes satisfying the resonance condition $\omega(k_\perp, k_\parallel) = k_\parallel v_\parallel$, where $v_\parallel$ is the axial velocity of the beam. The perpendicular wave vector, $k_\perp$, is determined from a Fourier analysis of the beam current in the perpendicular (radial) direction. For a beam of radial thickness a, $k_\perp$ lies in a narrow band about $\bar{k}_\perp \sim 2\pi/a$. These conditions are depicted geometrically in the three dimensional $(k_\parallel, k_\perp, \omega)$ space as shown in Figs. 2, 3, and 4 for a cold, collisionless plasma. Excited modes lie on the intersection of the $\omega = \omega(k_\parallel, k_\perp)$ and $\omega = k_\parallel v_\parallel$ surfaces, and have perpendicular wave vectors in the band about $\bar{k}_\perp$.

One of the high frequency electromagnetic modes, and the low frequency slow (or shear Alfvén) wave are sketched in Fig. 2. For clarity, the second high frequency mode has been omitted in the figure. Its surface is similar to the mode drawn. Beam and plasma dispersion surfaces fail to intersect so that these modes are not emitted by the beam. The high frequency modes have phase velocities greater than c, and do not interact with the fluid beam. The low frequency slow wave has its highest phase velocity in the small k or shear Alfvén region where the dispersion relation is $\omega = v_A k_\parallel$. Here, the parallel phase velocity is a constant v_A, and too slow to resonate with beam particles.

Figure 3 shows modes which are emitted by the beam. In a cold collisionless plasma there are only two: the intermediate frequency plasma oscillation-upper hybrid mode, and the low frequency fast wave. The dispersion surface for the plasma oscillation is very nearly the plane $\omega = \omega_p$. Emitted waves thus have a wavelength $\lambda \sim 2\pi(c/\omega_p)$, which in our case is a few millimeters. Since the beam head, which acts as the source of waves, occupies at least a ten centimeter region, we have a situation in which the source extends over many wavelengths of the emitted radiation. The response, therefore, accurately reproduces the source, and since the cold plasma wave group velocity is zero, the result is a disturbance localized to the beam head. Understanding this, we neglect the plasma wave. (This discussion ignores the presence of instabilities, since none occur with the rigid beam. In practice, the waves in the head region would give streaming instabilities a suprathermal start.)

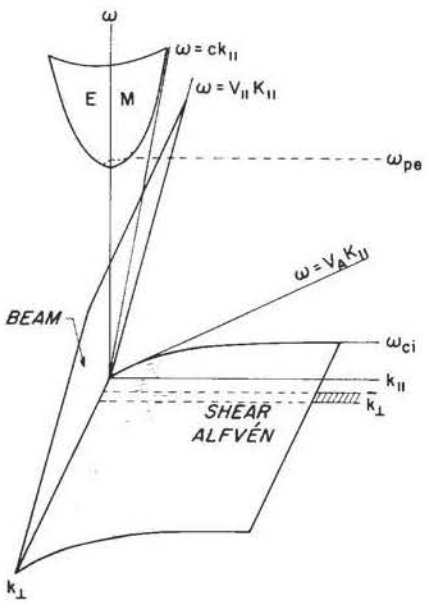

FIG. 2. Dispersion surfaces for high frequency electromagnetic mode and low frequency slow (shear Alfvén) mode. Beam surface for resonant, $\omega = k_\parallel v_\parallel$ interaction, is shown.

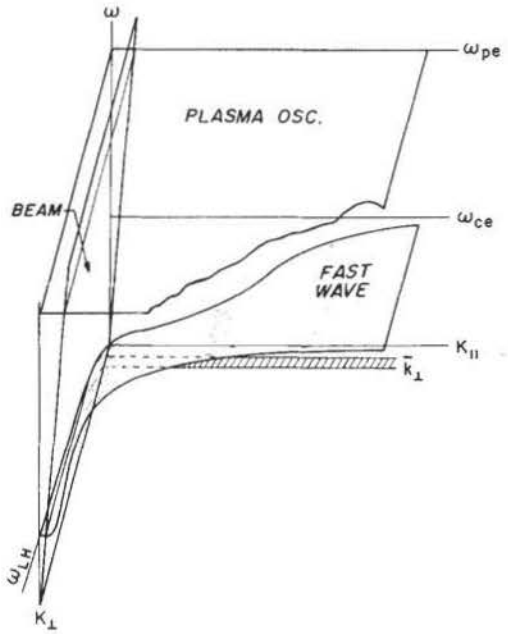

FIG. 3. Dispersion surfaces for plasma upper hybrid oscillation and low frequency, whistler-lower hybrid (fast) mode. Intersections with beam surface are shown.

Thus, we are left with the fast, low frequency wave for the plasma response. In different regions of wave vector and propagation angle, this mode is variously named "whistler," "compressional Alfvén," "lower hybrid," to cite a few. The surface of the mode is detailed, where it intersects the beam surface, in Fig. 4. Although the surface rises very steeply from the lower hybrid to the whistler mode as the propagation angle rotates from $\pi/2$, propagation is so close to perpendicular that the intersection curve is accurately given by the lower hybrid dispersion relation

$$\omega = v_A k_\perp (1 + k_\perp^2 c^2/\omega_p^2)^{-1/2} ;$$

and the appropriate $\bar{k}_\perp$ places the band of wave vectors on the weakly dispersive portion of this curve ($\bar{k}_\perp < \omega_p/c$).

Addition of temperature and collisional effects complicate the simple picture afforded by the cold fluid equations. For an initial plasma at 1 eV temperature, finite ion Larmor radius corrections are not significant; the magnetosonic, lower hybrid mode is given correctly by the cold fluid equations in the vicinity of $k_\perp \sim \bar{k}_\perp$.

Collision effects are never negligible since the plasma is initially cold and subsequently turbulent. At a sufficiently high collision frequency, the magnetosonic mode becomes critically damped and takes on the appearance of magnetic diffusion. It is this resistive medium response, appropriate to the parameters of a plasma heating experiment, which is considered in most detail. Two models for the dissipation are employed. The Langevin description of dissipation, employed by Chu and Rostoker,[5] using a friction term proportional to the individual species velocity, will be considered first. This leads most directly to easily interpreted results. Later, we treat the problem with friction terms conserving momentum between electron and ion species, as in classical transport theory; at high ν_{ei}, the plasma response is identical.

III. RETURN CURRENT EQUATIONS

A. Langevin friction

The discussion of the previous section reduces the problem to finding the steady long wavelength response of the plasma. Quantities depend only on the beam coordinate $\zeta = z - v_\parallel t$. The analysis is done first for a plasma described by cold, linearized, two fluid equations with Langevin dissipative terms

$$m_j \frac{\partial}{\partial t} \mathbf{v}_j = q_j \mathbf{E} + q_j \frac{\mathbf{v}_j \times \mathbf{B}_0}{c} - m_j \nu_j \mathbf{v}_j , \tag{1}$$

where $j = (e, i)$ for electrons and ions, B_0 is the applied field, and ν_j is the effective collision frequency.

Equation (1) may be solved for a plasma conductivity tensor, $\mathbf{J}_p = \sigma \cdot \mathbf{E}$, in the usual way. We simplify the expression by using the ordering

$$\nu_e/\Omega_e ,\ \Omega_i/\nu_i ,\ (m_e/m_i)^{1/2} \ll 1 ,$$

and neglecting the inertia terms. By anticipating the solution which will follow, one can show that the inertia terms are small, provided the time scale of the process, τ, obeys the inequalities

$$\nu_e \tau ,\ \nu_i \tau \gg 1 \text{ and } \nu_i \tau \gg \Omega_e \Omega_i / \nu_e \nu_i .$$

These conditions are well satisfied for the parameters appropriate to a plasma heating experiment (as indicated in Fig. 1).

The nonzero conductivity components are then:

Cross field conductivity:

$$\sigma_{rr} = \sigma_{\theta\theta} = \frac{\omega_e^2}{4\pi} \frac{\nu_e}{\Omega_e^2} \left(1 + \frac{\Omega_e \Omega_i}{\nu_e \nu_i}\right) \equiv \sigma_\perp ,$$

Hall conductivity:

$$\sigma_{r\theta} = -\sigma_{\theta r} = -\frac{\omega_e^2}{4\pi} \frac{1}{\Omega_e} \equiv -\sigma_H ,$$

Parallel conductivity:

$$\sigma_{zz} = \frac{\omega_e^2}{4\pi} \frac{1}{\nu_e} \equiv \sigma_\parallel . \tag{2}$$

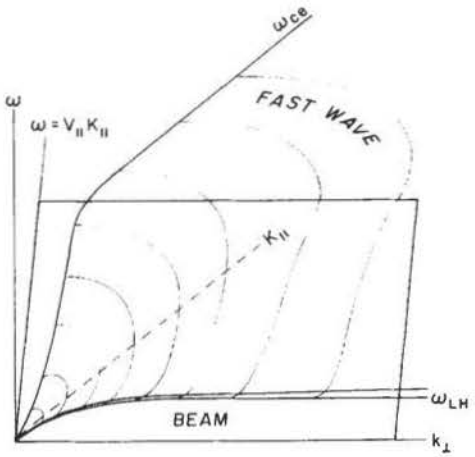

FIG. 4. Detail of beam interaction with fast wave.

The ion contribution enters the conductivity only through the second term of the factor $f \equiv 1 + \Omega_e \Omega_i / \nu_e \nu_i$ in $\sigma_\perp$. This is the term that was mentioned in the introduction and emphasized in Ref. 5. We shall consider it to be small ($f = 1.2$ for the parameters of Table I), in which case the ion response is negligible and both forms for the friction will give the same results. A highly collisionless state for the electrons, indicated by $\nu_e/\Omega_e \ll 1$ is the basic assumption. This is reflected in (6) where $\sigma_\perp$ is *proportional* to ν_e, showing that cross field currents are caused by collisions. It accounts for the ordering of conductivity coefficients

$$\sigma_\perp : \sigma_H : \sigma_\parallel = \epsilon^2 : \epsilon : 1, \tag{3}$$

and, ultimately, the slow decay of the theta current.

We replace $\mathbf{J}$ by $\mathbf{J} = \mathbf{J}_b + \mathbf{J}_p$ in Maxwell's equations

$$\nabla \times (\nabla \times \mathbf{E}) = -\frac{4\pi}{c^2}\frac{\partial}{\partial t}\mathbf{J} - \frac{1}{c^2}\frac{\partial^2}{\partial t^2}\mathbf{E}, \tag{4}$$

and eliminate $\mathbf{J}_p$ with the conductivity tensor. For the steady response, all z and t dependence may be combined into the single variable $\mathfrak{z} = z - v_\parallel t$. Identifying diffusion coefficients, $D \equiv c^2/4\pi\sigma$, this gives

$$\mathbf{e}_r\left(\gamma_\parallel^{-2}\frac{\partial^2}{\partial \mathfrak{z}^2}E_r - \frac{\partial^2}{\partial \mathfrak{z}\partial r}E_z + \frac{v_\parallel}{D_\perp}\frac{\partial}{\partial \mathfrak{z}}E_r - \frac{v_\parallel}{D_H}\frac{\partial}{\partial \mathfrak{z}}E_\theta = 0\right), \tag{5}$$

$$\mathbf{e}_\theta\left[\left(\frac{\partial^2}{\partial r^2} + \frac{1}{r}\frac{\partial}{\partial r} - \frac{1}{r^2}\right)E_\theta + \gamma_\parallel^{-2}\frac{\partial^2}{\partial \mathfrak{z}^2}E_\theta + \frac{v_\parallel}{D_\perp}\frac{\partial}{\partial \mathfrak{z}}E_\theta + \frac{v_\parallel}{D_H}\frac{\partial}{\partial \mathfrak{z}}E_r = -\frac{4\pi v_\parallel}{c^2}\frac{\partial}{\partial \mathfrak{z}}J_{b\theta}\right], \tag{6}$$

$$\mathbf{e}_z\left[\left(\frac{\partial^2}{\partial r^2} + \frac{1}{r}\frac{\partial}{\partial r}\right)E_z - \frac{v_\parallel^2}{c^2}\frac{\partial^2}{\partial \mathfrak{z}^2}E_z + \frac{v_\parallel}{D_\parallel}\frac{\partial}{\partial \mathfrak{z}}E_z = -\frac{4\pi v_\parallel}{c^2}\frac{\partial}{\partial \mathfrak{z}}J_{bz} + \frac{1}{r}\frac{\partial}{\partial r}r\frac{\partial}{\partial \mathfrak{z}}E_r\right], \tag{7}$$

$$\gamma_\parallel = (1 - v_\parallel^2/c^2)^{-1/2} \cong 1, \quad \text{for } v_\parallel/c \sim \tfrac{1}{10}.$$

To treat Eqs. (5)–(7) with some generality it is desirable to transform them into an algebraic system. This can be done for the present system with the appropriate Hankel transforms (in more general terms, the azimuthally symmetric form of the $\nabla \times \nabla \times$ operator in cylindrical geometry can be treated by this method). We apply the Hankel transformation defined by

$$\mathfrak{f}_m(k_\perp) = \int_0^\infty dr\, r J_m(k_\perp r) f(r) \equiv \mathfrak{F}_m[f] \tag{8}$$

$$f(v) = \int_0^\infty dk_\perp\, k_\perp J_m(k_\perp r)\, \mathfrak{f}_m(k_\perp)$$

using the kernal $J_1(k_\perp r)$ on (5), (6) and the kernal $J_0(k_\perp r)$ on (7). Some of the details of the Hankel transform algebra are given in Appendix I. Basically, the J_0 transform on $(1/r)(\partial/\partial r)rE_r$ in Eq. (7) is converted into a J_1 transform by the radial operator, while the opposite process occurs on the $(\partial/\partial r)E_z$ terms of Eq. (5). Thus, the system remains closed (no new J_m with $m \neq 0, 1$, transforms are introduced). Also, using a conventional Fourier transform on the $\mathfrak{z}$ variable, we obtain

$$\mathbf{D}(k_\perp, k_\parallel)\boldsymbol{\mathcal{E}} = \mathscr{S}, \tag{9}$$

where the field transforms are

$$\begin{pmatrix}\mathcal{E}_z(k_\perp)\\ \mathcal{J}_z(k_\perp)\end{pmatrix} = \mathfrak{F}_0\left[\begin{pmatrix}E_z(r)\\ J_z(r)\end{pmatrix}\right]$$

$$\begin{pmatrix}\mathcal{E}_{\theta,r}(k_\perp)\\ \mathcal{J}_\theta(k_\perp)\end{pmatrix} = \mathfrak{F}_1\left[\begin{pmatrix}E_{\theta,r}(r)\\ J_\theta(r)\end{pmatrix}\right]. \tag{10}$$

The source is given by

$$\mathscr{S} = -i(4\pi v_\parallel k_\parallel/c^2)\mathcal{J}, \tag{11}$$

and the dispersion matrix is

$$\mathbf{D} = \begin{bmatrix} -k_\parallel^2 + ik_\parallel\frac{v_\parallel}{D_\perp} & -ik_\parallel\frac{v_\parallel}{D_H} & ik_\parallel k_\perp \\ ik_\parallel\frac{v_\parallel}{D_H} & -k_\perp^2 - k_\parallel^2 + ik_\parallel\frac{v_\parallel}{D_\perp} & 0 \\ -ik_\parallel k_\perp & 0 & -k_\perp^2 + \frac{v_\parallel^2}{c^2}k_\parallel^2 + ik_\parallel\frac{v_\parallel}{D_\parallel} \end{bmatrix}. \tag{12}$$

To find the normal modes, we make use of the ordering

$$D_\parallel : D_H : D_\perp = \epsilon^2 : \epsilon : 1,$$

which follows from Eq. (3), and also assume that $k_\parallel(D_\perp/v_\parallel) \ll 1$. This latter restriction follows from the Sec. II conclusion that only long axial wavelengths are relevant, and will be self-consistently verified by the solution. These simplifications lead to the factorization of $D \equiv \det D$,

$$D = -ik_\parallel v_\parallel \frac{1}{D_\parallel D_H^2}(k_\parallel v_\parallel + ik_\perp^2 D_\parallel)\left(k_\parallel v_\parallel + ik_\perp^2\frac{D_H^2}{D_\perp}\right) \tag{13}$$

and hence, from $D = 0$, to two "diffusion" normal modes.

Equation (9) for the fields is easily inverted, and we find

$$\mathcal{E}_\theta = D^{-1}[A_{\theta\theta}\mathcal{S}_\theta + A_{\theta z}\mathcal{S}_z] \tag{14}$$

$$\mathcal{E}_z = D^{-1}[A_{z\theta}\mathcal{S}_\theta + A_{zz}\mathcal{S}_z] \tag{15}$$

with the relevant adjoint matrix components, neglecting order $k_\parallel^2/k_\perp^2$ terms, given by

$$\begin{aligned} A_{\theta\theta} &= -k_\parallel(v_\parallel/D_\perp D_\parallel)(k_\parallel v_\parallel + ik_\perp^2 D_\parallel), \\ A_{\theta z} = A_{z\theta} &= -k_\parallel^2 k_\perp(v_\parallel/D_H), \\ A_{zz} &= -k_\parallel(v_\parallel/D_H^2)[k_\parallel v_\parallel + ik_\perp^2(D_H^2/D_\perp)]. \end{aligned} \tag{16}$$

For the cases of interest, the cross terms in (14) are small corrections, and the return currents are described by decoupled diffusion equations. Thus, the ratio of the second to the first term in Eq. (14) is

$$\frac{\mathcal{E}_\theta^{(z)}}{\mathcal{E}_\theta^{(\theta)}} = \frac{\mathcal{S}_z}{\mathcal{S}_\theta}\frac{k_\parallel k_\perp}{(D_H/D_\perp)[-k_\perp^2 + ik_\parallel(v_\parallel/D_\parallel)]} \sim \frac{\mathcal{S}_z}{\mathcal{S}_\theta}\frac{1}{\epsilon}\frac{k_\parallel}{k_\perp}, \tag{17}$$

and always small for $\mathcal{S}_\theta \geq \mathcal{S}_z$, $k_\parallel/k_\perp \lesssim \epsilon^2$. Similarly, in Eq. (15), we assume

$$\frac{\mathcal{E}_\theta^{(\theta)}}{\mathcal{E}_z^{(z)}} \sim \frac{1}{\epsilon}\frac{k_\parallel}{k_\perp}\frac{\mathcal{S}_\theta}{\mathcal{S}_z} \ll 1, \tag{18}$$

although this is generally larger than the ratio (17), and there are practical cases when (18) will not be satisfied. In those cases, the axial return current would be driven more by $J_{B\theta}$ than by J_{Bz}. Since, how-

ever, the axial return current plays a negligible role in the most important results, we will treat only the simpler case.

We are now left with

$$\mathcal{E}_\theta = -i(D_H^2/D_\perp)[k_\parallel v_\parallel + ik_\perp^2(D_H^2/D_\perp)]^{-1}S_\theta\,, \tag{19}$$

$$\mathcal{E}_z = -iD_\parallel(k_\parallel v_\parallel + ik_\perp D_\parallel^2)^{-1}S_z\,. \tag{20}$$

The equation for the radial electric field is identical to (19), apart from a constant factor. $\mathcal{E}_r$ and $\mathcal{E}_\theta$ are thus the different components of the angular return current mode, the polarization being

$$\mathcal{E}_r = (\sigma_H/\sigma_\perp)\mathcal{E}_\theta\,. \tag{21}$$

These equations can be re-expressed in a more understandable form. We write the fields in terms of the plasma currents with Ohm's law and return to the differential equation description by inverting the transforms.

$$\frac{D_H^2}{D_\perp}\left(\frac{\partial^2}{\partial r^2}+\frac{1}{r}\frac{\partial}{\partial r}-\frac{1}{r^2}\right)J_{p\theta}+v_\parallel\frac{\partial}{\partial\zeta}J_{p\theta}=-v_\parallel\frac{\partial}{\partial\zeta}J_{b\theta}\,, \tag{22}$$

and

$$D_\parallel\left(\frac{\partial^2}{\partial r^2}+\frac{1}{r}\frac{\partial}{\partial r}\right)J_{pz}+v_\parallel\frac{\partial}{\partial\zeta}J_{pz}=-v_\parallel\frac{\partial}{\partial\zeta}J_{bz}\,, \tag{23}$$

are the basic equations for the angular and axial return currents.

B. Momentum conserving friction

The previous subsection has considered the interaction from the standpoint of cold two-fluid equations with Langevin dissipative terms. Collision frequencies were phenomenological and estimates (Table I) made for them were anomalously high. Indeed, even the Langevin form is anomalous in that classical collisional dissipation conserves momentum between electron and ion fluids, whereas the Langevin form does not. Of course, the electron plus ion fluid momentum does not have to be conserved in the dissipative process. Other components, such as waves, external magnetic field, and even beam electrons can absorb momentum. This becomes more likely when noncollisional processes account for the dissipation. However, the classical form of the collision term is a possibility, so we now consider its consequences for the rotating beam-plasma interaction.

Starting equations for the plasma response are thus

$$m_e\frac{d}{dt}\mathbf{v}_e = -e\mathbf{E}-\frac{e}{c}\mathbf{v}_e\times\mathbf{B}-m_e\nu_{ei}(\mathbf{v}_e-\mathbf{v}_i)\,, \tag{24}$$

$$m_i\frac{d}{dt}\mathbf{v}_i = e\mathbf{E}+\frac{e}{c}\mathbf{v}_i\times\mathbf{B}-m_e\nu_{ei}(\mathbf{v}_i-\mathbf{v}_e)\,. \tag{25}$$

The result of classical transport theory[8,7] is slightly different from this in that the friction coefficient parallel to the applied field is a factor of 2 smaller than the cross field coefficient. For simplicity, the friction coefficients here are taken to be isotropic. Modifications required to use the classical form are straightforward and can easily be made later.

Equations (24) and (25) can be re-arranged to give the linearized, cold magnetohydrodynamic equations

Momentum equation:

$$m_i n\frac{\partial}{\partial t}\mathbf{V}=\frac{1}{c}\mathbf{J}\times\mathbf{B} \tag{26}$$

Ohm's law:

$$\frac{4\pi}{\omega_{pe}^2}\frac{\partial}{\partial t}\mathbf{J}=\mathbf{E}+\frac{1}{c}\mathbf{V}\times\mathbf{B}-\frac{1}{nec}\mathbf{J}\times\mathbf{B}-\eta\mathbf{J}\,. \tag{27}$$

Here, $\mathbf{V}=m_i\mathbf{v}_i+m_e\mathbf{v}_e$, $\mathbf{J}=ne(\mathbf{v}_i-\mathbf{v}_e)$, $\eta=\nu_{ei}m_e/ne^2$, and order m_e/m_i terms have been dropped. Qualitative differences between these and Eqs. (1) quickly become apparent. For example, the response to (26) and (27) has $\mathbf{J}\times\mathbf{B}=0$, so no net current flows across the magnetic field. In spite of this the same behavior as previously can result from these equations under certain conditions. Here, the response is interpreted as a critically damped magnetosonic wave, but the appearance is that of magnetic diffusion.

After a Fourier transform in time, Eqs. (26) and (27) may be solved for the conductivity tensor. Using the same convention as in Eq. (2), the coefficients are

$$\begin{aligned}
\sigma_\perp &= \frac{\omega_p^2}{4\pi}\left[\nu_{ei}-i\omega\left(1-\frac{\Omega_e\Omega_i}{\omega^2}\right)\right]\left\{\left[\nu_{ei}-i\omega\left(1-\frac{\Omega_e\Omega_i}{\omega^2}\right)\right]^2+\Omega_e^2\right\}^{-1}\,,\\
\sigma_h &= \frac{\omega_p^2}{4\pi}\,\Omega_e\left\{\left[\nu_{ei}-i\omega\left(1-\frac{\Omega_e\Omega_i}{\omega^2}\right)\right]^2+\Omega_e^2\right\}^{-1}\,,\\
\sigma_\parallel &= \frac{\omega_p^2}{4\pi}\frac{1}{\nu_{ei}-i\omega}\,.
\end{aligned} \tag{28}$$

From the discussion of Sec. II, it follows that only the low frequency response need be considered and that modes excited by the beam will propagate nearly perpendicular to the applied field. In forming the plasma dielectric tensor, $\boldsymbol{\epsilon}=\mathbf{I}-(4\pi i/\omega)\sigma$, the identity tensor part may be neglected, so that

$$\boldsymbol{\epsilon}=-\frac{4\pi i}{\omega}\sigma\,, \tag{29}$$

and the plasma modes are given by

$$\mathbf{n}\times(\mathbf{n}\times\mathbf{E})+\boldsymbol{\epsilon}\cdot\mathbf{E}=0=\begin{bmatrix}\epsilon_\perp & \epsilon_H & 0\\ -\epsilon_H & \epsilon_\perp-n^2 & 0\\ 0 & 0 & \epsilon_\parallel\end{bmatrix}\begin{bmatrix}E_r\\ E_\theta\\ E_z\end{bmatrix}\,, \tag{30}$$

where $n=k_\perp c/\omega$ is the refractive index.

The Hankel transform formalism has been used, but we have not transformed to beam frame variables or taken the asymptotic $\omega\to 0$ limit. The dispersion relation and the polarization are given by

$$-n^2\epsilon_\perp+\epsilon_\perp^2+\epsilon_H^2=0\,, \tag{31}$$

$$E_r/E_\theta=-\epsilon_H/\epsilon_\perp=-\sigma_H/\sigma_\perp\,. \tag{32}$$

Equation (31) can be solved without further approximation, and we find

$$\omega=\left[2\left(1+\frac{\omega_p^2}{k^2c^2}\right)\right]^{-1}\left\{-i\nu_{ei}\pm\left[4\omega_{lh}^2\left(1+\frac{\omega_p^2}{k^2c^2}\right)-\nu_{ei}^2\right]^{1/2}\right\}, \tag{33}$$

with $\omega_{lh}^2=\Omega_e\Omega_i$, the lower hybrid frequency.

If $\nu_{ei}<2\omega_{lh}$, the mode has a wave character, with

some damping, for all k. As $\nu_{ei} \to 0$ the usual magnetosonic-lower hybrid dispersion relation is obtained

$$\omega = \pm \omega_{lh}(1 + \omega_p^2/k^2c^2)^{-1/2}. \tag{34}$$

When $\nu_{ei} > 2\omega_{lh}$, the mode will be critically damped at sufficiently large wavenumber. If

$$\nu_{ei} \gg 2\omega_{lh}(1 + \omega_p^2/k^2c^2)^{1/2}, \tag{35}$$

the two modes are

$$\omega = -i[\nu_{ei}(1 + \omega_p^2/k^2c^2)^{-1}], \quad -i(\omega_{lh}^2/\nu_{ei}).$$

Furthermore, when $\omega_p^2 \gg k^2c^2$, the first mode becomes $\omega = -i\nu_{ei}(c^2/\omega_p^2)k^2$, which is the dispersion relation for diffusion. The second mode is an evanescent, nonpropagating response which, in practice, damps out a few centimeters behind the beam bead.

For the critically damped diffusion case, the mode polarization is

$$E_r/E_\theta = -\Omega_e/\nu_{ei}, \tag{36}$$

which is equivalent to Eq. (28), when the ion response is negligible. Without repeating the calculation, it is clear that when (35) applies, the results will be the same as those of the previous subsection, excepting the ion contribution to $\sigma_\perp$ in Eq. (2). Thus, the basic response is the same with both models for the friction, but the unusual ion term noted in Ref. 5, results only when the Langevin friction is used.

When the mode is not critically damped, a different plasma response results from these equations. The beam emits magnetosonic waves. An accurate calculation of this phenomena, however, is not very tractable, for a number of reasons. Wavelengths implied by the resonance condition $\omega = k_\parallel v_\parallel$ tend to be longer than the system in cases of practical interest. The mode period $\omega^{-1} \cong 1/k_\perp V_A$ is longer than either the beam pulse length or the time expected for the beam to stop. This makes the problem inherently a transient one and in addition, invalidates a test particle type calculation. Chu *et al.*[8] have considered the problem by neglecting beam propagation and treating the beam as a rising and falling current pulse. In this way they obtain estimates of emitted wave energy but cannot determine the drag force on a propagating beam. Our viewpoint, in this case, is that the current neutralization and beam trapping can occur from the electron interaction alone, and that a significant ion response will develop only on a longer time scale [as considered in (II)]. Thus, we estimate the drag force on the beam in the same way, as in the critically damped case, taking $m_i \to \infty$, of course.

The parameters in Table I imply

$$\omega_{lh} = 5 \times 10^8 \text{ sec}^{-1},$$

$$\omega_p/kc \cong 3 \quad (k = 2\pi),$$

so that $\nu_{ei} \cong 2\omega_{lh}$. The collision frequency $\nu_{ei} \sim 10^9$ corresponds to the Sagdeev[9] estimate $\nu_{ei} \sim 0.1\omega_{pi}$, for $n_p = 10^{14}$. An intense beam may result in strong turbulence and give an effective ν higher than this. For example, recent experiments at Physics International[10] seem to indicate numbers in the range $\nu_{ei} \sim 3 \times 10^9 - 1.5 \times 10^{10}$ (when scaled linearly to $n_p = 10^{14}$). Simulations of Thode[11] show $\nu_{ei} \sim 0.2 - 0.4\omega_{pi}$. Other experiments[12] give $\nu_{ei} \sim 0.1\omega_{pi}$, while some[13] are considerably less.

IV. RETURN CURRENT PROPERTIES

A. Infinite medium solution

We first take an example where the conducting wall bounding the plasma is sufficiently far from the beam so that its effect may be neglected. In this case the return current equations (29) and (30) are easily solved for the plasma currents when the beam current is known. We specify the beam current distribution to be

$$J_{b\theta} = I_{b\theta}(2/a^2)r \exp(-r^2/a^2)H(-\xi) \tag{37}$$

$$J_{bz} = I_{bz}(1/\pi a^2) \exp(-r^2/a^2)H(-\xi), \tag{38}$$

where $H(\xi)$ is the unit step function. $I_{b\theta}$ as defined by

$$I_{b\theta} \equiv \int_0^\infty J_{b\theta}\, dr \tag{39}$$

is current per unit length, whereas

$$I_{bz} \equiv \int_0^\infty 2\pi r\, dr J_{bz} \tag{40}$$

is the total axial current.

The current distributions (37) and (38) correspond physically to a beam with a Gaussian density profile rotating rigidly about the cylinder axis and propagating along z. Such a beam is considerably less annular than those encountered in practice. This form is used here as a model to exhibit the return current properties more clearly. The use of a sharp rising step function, front-to-beam produces a corresponding step in the return currents which is, strictly speaking, in violation of previous smoothness assumptions on the axial variations. That the smoothing of this step of the amount required for logical consistency has a negligible effect, will be made clear in a following section.

We then find for the plasma response

$$J_{p\theta} = -I_{b\theta}2r\{a[1 - (z - v_\parallel t)/l_\perp]\}^{-2} \times \exp(-r^2\{a^2[1 - (z - v_\parallel t)/l_\perp]\}^{-1})H(-z + v_\parallel t), \tag{41}$$

and

$$J_{pz} = -I_{bz}\{\pi a^2[1 - (z - v_\parallel t)/l_\parallel]\}^{-1} \times \exp(-r^2\{a^2[1 - (z - v_\parallel t)/l_\parallel]\}^{-1})H(-z + v_\parallel t), \tag{42}$$

and the solutions are expressed in the laboratory variables. Length parameters, $l_\perp$ and $l_\parallel$, for the return current decay, are given by

$$l_\parallel = \left(\frac{a\omega_{pe}}{2c}\right)^2 \frac{v_\parallel}{\nu_e}, \tag{43}$$

$$l_\perp = \left(\frac{a\omega_{pe}}{2c}\right)^2 \frac{v_\parallel}{\nu_e} \frac{1}{1 + (\Omega_e\Omega_i/\nu_e\nu_i)}, \tag{44}$$

where $l_\parallel$ and $l_\perp$ are approximately 300 cm for $a = 1$ cm and $\Omega_e\Omega_i/\nu_e\nu_i \ll 1$.

This distance in which the axial current decays is quite long (the order of the beam length in a 100 nsec pulse). This is expected from the high parallel conductivity. However, the angular, cross-field current de-

cays in the same length (when ion motion is neglected). To give an account of this we again consider Ohm's law,

$$J_r = \sigma_\perp E_r - \sigma_H E_\theta ,$$

$$J_\theta = \sigma_H E_r + \sigma_\perp E_\theta .$$

Specification of the electrical boundary conditions holding across the beam gives a single relation between J_θ and E_θ in terms of an effective cross-field conductivity. Requiring the gap between inner and outer surfaces of the annulus to be open circuit implies $J_r = 0$, $E_r = (\sigma_H/\sigma_\perp)E_\theta$ [this is just Eq. (21)], or

$$J_\theta = \sigma_f E_\theta + O(\epsilon^2), \text{ where } \sigma_f \equiv (\sigma_H/\sigma_\perp)\sigma_H , \tag{45}$$

which shows why the effective diffusion coefficient for the angular return current is $D_f = D_H^2/D_\perp$, and this explains the long decay length. The open circuit prevents charge from being drawn off at the edges so E_r builds up until the magnetic $\mathbf{V}_\theta \times \mathbf{B}_z$ force is nullified. In the highly collisionless case, the effective cross field conductivity then assumes the unmagnetized value

$$\sigma_f = \frac{\omega_e^2}{4\pi\nu_e}\left(1 + \frac{\Omega_e\Omega_i}{\nu_e\nu_i}\right) = \frac{\sigma_\parallel}{f}, \tag{46}$$

where f is $O(1)$.

The total axial return current is given by

$$I_{bz} \equiv \int_0^\infty 2\pi r\, dr\, J_{bz} = -I_{bz} H(-z + v_\parallel t), \tag{47}$$

so there is no net decay. By contrast the total angular return current (per unit length) is

$$I_{b\theta} \equiv \int_0^\infty dr\, J_b = -I_{b\theta}[1 - (z - v_\parallel t)/l_\perp]^{-1} H(-z + v_\parallel t) \tag{48}$$

which does decay.

B. Disposition of beam energy

The energy lost by the beam electrons can be traced as follows. We first take the axial current and compute

$$\int_0^\infty J_{bz} E_z 2\pi r\, dr = \frac{I_b^2}{\sigma_\parallel 2\pi a^2}\left(1 - \frac{z}{2l_\parallel}\right)^{-1}, \tag{49}$$

$$\int_0^\infty \frac{J_{bz}^2}{\sigma_\parallel} 2\pi r\, dr = \frac{I_b^2}{\sigma_\parallel 2\pi a^2}\left(1 - \frac{z}{l_\parallel}\right)^{-1}, \tag{50}$$

where the beam energy not lost to Ohmic heating of the plasma goes into the magnetic field. We see that for $-z \ll l_\parallel$ all the beam energy is dissipated in the plasma while for $-z \gg l_\parallel$ it is partitioned equally between the magnetic field and Ohmic heating.

For the angular current

$$\int_0^\infty J_{b\theta} E_\theta 2\pi r\, dr = \pi \frac{I_{b\theta}^2}{\sigma_f}\left(1 - \frac{z}{2l_\perp}\right)^{-2}, \tag{51}$$

$$\int_0^\infty \frac{J_{p\theta}^2}{\sigma_f} 2\pi r\, dr = \pi \frac{I_{b\theta}^2}{\sigma_f}\left(1 - \frac{z}{l_\perp}\right)^{-2} . \tag{52}$$

I_b is dimensioned as current per unit length so that dimensional discrepancy between (49), (50), and (51), (52) is only apparent. All formulae give power per unit length.

For short distances behind the beam head, $-z \ll l_\perp$, beam energy still goes into the plasma; but for large distances, $-z \gg l_\perp$, one fourth goes into the plasma and three fourths to the magnetic field energy. This results from the net decay of the angular current.

C. Finite beam rise time

The beam current distribution previously used for the angular current, Eq. (37), perfectly represented sharp or zero rise time pulses. To generalize the formulae, the beam current axial dependence is modified.

$$I_{b\theta} \to \begin{cases} 0, & 0 < \vartheta, \\ -(\vartheta/l_r) I_{b\theta}, & -l_r \le \vartheta \le 0, \\ I_{b\theta}, & \vartheta < -l_r, \end{cases} \tag{53}$$

where $l_r = v_\parallel t_r$ is the rise length (t_r is the rise time as given, for instance, from the diode trace). The source goes like $\partial I_{b\theta}/\partial\vartheta$, i.e., Eq. (6), hence, is $-I_{b\theta}/l_r$ in the region $-l_r \le \vartheta \le 0$, and zero otherwise. With the identification $\vartheta = z - v_\parallel t \to \vartheta - \vartheta'$, Eq. (41) may be used as a Green's function to calculate the finite rise time expression.

$$J_{p\theta} = -\frac{2I_{b\theta} l_\perp}{r l_r}\int_{-l_r}^{0} r^2 d\vartheta' \left\{ l_\perp a^2 \left[1 - \left(\frac{\vartheta - \vartheta'}{l_\perp}\right)\right]^2 \right\}^{-1} \times \exp\left(r^2 \left\{ a^2 \left[1 - \left(\frac{\vartheta - \vartheta'}{l_\perp}\right)\right]\right\}^{-1}\right). \tag{54}$$

This applies for $\vartheta \le -l_r$, or behind the rising portion of the beam. When $-l_r \le \vartheta \le 0$, the appropriate lower limit of integration would be ϑ. Thus,

$$J_{p\theta} = \frac{2I_{b\theta} l_\perp}{r l_r}\left[\exp\left(-\frac{r^2}{a^2(1 - \vartheta/l_\perp)}\right) - \exp\left(-\frac{r^2}{a^2(1 - (\vartheta + l_r)/l_\perp)}\right)\right] . \tag{55}$$

A more useful form, is obtained by expanding for small $l_r/l_\perp$. Also, putting $\vartheta = x - l_r$, so that minus x measures the distance behind the rising portion of the beam, we find,

$$J_{p\theta} = -\frac{I_{b\theta} 2r}{a^2(1 - x/l_\perp)} \exp\left\{ -r^2 \left[a^2 \left(1 - \frac{x}{l_\perp}\right)\right]^{-1}\right\} \times \left[1 - \frac{l_r}{l_\perp}\frac{1}{(1 - x/l_\perp)}\left(1 - \frac{1}{2}\frac{r^2}{a^2(1 - x/l_\perp)}\right)\right]. \tag{56}$$

Equation (41) is recovered, as it must be, in the $l_r \to 0$ limit. The behavior indicated by (56) is as expected for a diffusion process. By the time the beam current reaches its full value, the initial portion of return current will have already begun to diffuse. Thus at $x = 0$, by comparison with the zero rise length case at $\vartheta = 0$, the return current is less for $r < \sqrt{2}a$, and greater for $r > \sqrt{2}a$.

For the effect on total return current, (55) may be integrated over r. Alternately, Eq. (48) can be applied as a Green's function to calculate this directly. In either case the result is

$$I_{p\theta} = -I_{b\theta}(l_\perp/l_r)\ln\{(1 - \vartheta/l_\perp)[1 - (\vartheta + l_r)/l_\perp]^{-1}\} . \tag{57}$$

The maximum return current is attained at $\vartheta = -l_r$, so,

$$I_{p\theta} \lesssim -I_{b\theta}\frac{l_\perp}{l_r}\ln\left(1+\frac{l_r}{l_\perp}\right)$$
$$\cong -I_{b\theta}\left(1-\frac{1}{2}\frac{l_r}{l_\perp}\right), \text{ for } \frac{l_r}{l_\perp}\lesssim\frac{1}{2}. \quad (58)$$

Here, the distinctive feature of the theta current, that it undergoes a net decay, is most evident. This decay competes with the rise of the beam current and limits the maximum theta return current to less than the full neutralizing value.

By comparison, no rise time limitations are placed on the axial counter current. Although the current distribution is affected by the details of the pulse shape, and there will be premature diffusion of the initial return current pulse, the net axial counter current will always reach the full neutralizing value.

In practice, the limitation imposed by (58) is not severe, owing to the magnitude of $l_\perp$. For a rise time of approximately 10 nsec, $l_r/l_\perp \sim \frac{1}{10}$, and the loss of maximum is only 5%. If the decay length were determined by the cross field conductivity, $\sigma_\perp$, the same rise time would give $l_r/l_\perp \sim 40$, and a reduction in the current maximum of 90%.

D. Conducting boundary

When the plasma is enclosed by a cylindrical conductor, the derivation of the diffusion equations in Sec. III still applies. Thus,

$$\frac{D_\parallel}{v_\parallel}\left(\frac{\partial^2}{\partial r^2}+\frac{1}{r}\frac{\partial}{\partial r}\right)J_{pz}+\frac{\partial}{\partial\vartheta}J_{pz}=-\frac{\partial}{\partial\vartheta}J_{bz}, \quad (59)$$

$$\frac{D_H^2}{D_\perp v_\parallel}\left(\frac{\partial^2}{\partial r^2}+\frac{1}{r}\frac{\partial}{\partial r}-\frac{1}{r^2}\right)J_{p\theta}+\frac{\partial}{\partial\vartheta}J_{p\theta}=-\frac{\partial}{\partial\vartheta}J_{b\theta}, \quad (60)$$

are to be solved, subject to the appropriate boundary conditions at $r=b$, the conductor radius. Recall that $\vartheta = z - v_\parallel t$ is the beam frame axial variable. The electrical boundary conditions $E_z=0$, $E_\theta=0$ imply $J_{pz}=0$ and $J_{p\theta}=0$, because of the Ohm's law relation.

For a step front beam with current distribution

$$J_{bz}=I_{bz}H(-\vartheta)f_\parallel(r),$$
$$J_{b\theta}=I_{b\theta}H(-\vartheta)f_\perp(r), \quad (61)$$

the solutions are

$$J_{pz}=-I_{bz}H(-\vartheta)\sum_{m=1}^{\infty}\exp(k_m^\parallel\vartheta)\frac{2S_m^\perp}{b^2J_1^2(x_{0m})}J_0\left(\frac{x_{0m}}{b}r\right), \quad (62)$$

$$J_{p\theta}=-I_{b\theta}H(-\vartheta)\sum_{m=1}^{\infty}\exp(k_m^\parallel\vartheta)\frac{2S_m^\parallel}{b^2J_2^2(x_{1m})}J_0\left(\frac{x_{1m}}{b}r\right), \quad (63)$$

where x_{0m}, x_{1m} are the roots of J_0 and J_1. Decay decrements are given by

$$k_m^\parallel=\frac{x_{0m}^2}{b^2}\frac{D_\parallel}{v_\parallel},$$
$$k_m^\perp=\frac{x_{1m}^2}{b^2}\frac{D_f}{v_\parallel}, \quad (64)$$

with source components

$$s_m^\parallel=\int_0^b dr\, rJ_0\left(\frac{x_{0m}}{b}r\right)f_\parallel(r),$$
$$s_m^\perp=\int_0^b dr\, rJ_1\left(\frac{x_{1m}}{b}r\right)f_\perp(r). \quad (65)$$

For short distances behind the beam head $|k_1\vartheta|\lesssim 1$, the complete series is needed, and it is then more convenient to use the solutions (41) and (42) which neglect the boundaries. When $|k_1\vartheta|\gg 1$, the series can be approximated by their first terms

$$J_{pz}=-I_{bz}H(-\vartheta)\exp(k_1^\parallel\vartheta)\frac{2S_1^\parallel}{b^2J_1^2(x_{01})}J_0\left(\frac{x_{01}}{b}r\right), \quad (66)$$

$$J_{p\theta}=-I_{b\theta}H(-\vartheta)\exp(k_1^\perp\vartheta)\frac{2S_1^\perp}{b^2J_2^2(x_{11})}J_1\left(\frac{x_{11}}{b}r\right). \quad (67)$$

It is evident from this that the net axial counter current decays due to the boundary. In this case the difference between the beam current and the return current flowing in a plasma will be carried by the conducting wall. Similar remarks apply to the angular current, although [see Eq. (48)] this current decays even without boundaries.

When finite beam rise time is considered, the boundaries limit the maximum return currents

$$I_{pz}\lesssim -I_{bz}(l_1^\parallel/l_r)[1-\exp(-l_r/l_1^\parallel)], \quad (68)$$

$$I_{p\theta}\lesssim -I_{b\theta}(l_1^\perp/l_r)[1-\exp(-l_r/l_1^\perp)]. \quad (69)$$

l_r is the beam rise length and $l_1^\parallel=(k_1^\parallel)^{-1}$ and $l_1^\perp=(k_1^\perp)^{-1}$ are decay lengths for the finite boundary case. For small l_r/l_1, Eqs. (68) and (69) coincide with (58) which applied to the angular current in infinite medium.

V. STOPPING POWER

As a result of the interaction, beam electrons experience a drag force

$$F_\parallel=-e\left(E_z-\frac{v_\perp}{c}B_r\right). \quad (70)$$

B_r is readily determined from Faraday's law as

$$B_r(\vartheta)=-\frac{c}{v_\parallel}E_\theta(\vartheta), \quad (71)$$

where $\vartheta = z - v_\parallel t$ is the coordinate following the beam. Taking values from immediately behind the beam head, we find

$$F_\parallel=e\frac{v_\perp}{v_\parallel}\frac{\sigma_\perp}{\sigma_H^2}J_{b\theta}=-\frac{n_b}{n_p}\frac{mc^2}{v_\parallel}\nu_e f \ (v_\perp\cong c), \quad (72)$$

and the contribution from the axial return current has been neglected as being of order $(v_\parallel/v_\perp)^2$. The drag force is increased over that for a nonrotating beam by the factor $(c/v_\parallel)f$.

From (71) it follows that $F_\perp=-e[E_\theta+(v_\parallel/c)B_r]=0$; there are no torques. This is a result familiar from the resistive ring concept for trapping rotating beams as proposed by Christofilos in the astron.[14] It is, however, a direct consequence of the steady state calculation (Faraday's law, independent of any interaction, is sufficient to determine this). Some torque may develop during the trapping phase.

Assuming no torques, the perpendicular momentum is conserved, and the energy lost during trapping will be

$$E = mc^2\left[\left(1+\frac{p_\perp^2+p_\parallel^2}{m^2c^2}\right)^{1/2} - \left(1+\frac{p_\perp^2}{m^2c^2}\right)^{1/2}\right] \cong \tfrac{1}{2}\gamma m v_\parallel^2 . \qquad (73)$$

This implies a stopping length

$$l_s = \frac{1}{2}\frac{n_p}{n_b}\left(\frac{v_\parallel}{c}\right)^3 \frac{\gamma}{f}\frac{c}{\nu_e}, \qquad (74)$$

which is a factor approximately $(v_\parallel/c)^3$ smaller than for nonrotating beams.

Magnetic field dependence of the drag force enters only through the factor $f = 1 + \Omega_e\Omega_i/\nu_e\nu_i$. This is another consequence of the form assumed by the effective cross field conductivity, $\sigma_f = \sigma_H^2/\sigma_\perp$. $F_\parallel$, accordingly, is almost B independent, for example, with the assumed parameters, $\Omega_e\Omega_i/\nu_e\nu_i = \frac{1}{5}$.

To summarize, we find the angular counter current of a rotating beam to be similar in many respects to the usual return current.[1] In particular, for the parameters of a typical plasma heating experiment, angular current neutralization may, to a good approximation, be considered as complete. The fields acting on the beam may then be calculated simply using the neutralizing condition $\mathbf{J}_p = -\mathbf{J}_b$ in conjunction with Ohm's law, $\mathbf{J}_p = \sigma_\parallel \mathbf{E}$, with $\sigma_\parallel \equiv \omega_{pe}/4\pi\nu_e$.

The primary difference, and also the feature of most importance, is the stopping power anomaly, which is greatly enhanced for the rotating beam. For example, the Table I parameters imply a rotating beam stopping length of 30 cm, and this is for a beam-to-plasma density ratio of 10^{-3}. Without the rotation, the stopping length, due to the axial return current alone would be 3×10^4 cm. Thus, a plasma which is transparent to a straight beam will completely stop a rotating beam. By transfering the rotational of the beam in a second stage [as treated in (II) and taking a fraction of a microsecond], the plasma can then absorb all the beam energy.

ACKNOWLEDGMENTS

We would like to thank G. Benford, W. C. Condit, F. Dothan, A. Fisher, C. W. Roberson, and T. Tajima for their discussions of this problem.

This work was supported in part by Energy Research and Development Administration, contracts AT(04-3)34 PA207 (University of California, Irvine) and E(11-1)-3070 (Massachusetts Institute of Technology).

APPENDIX–HANKEL TRANSFORM ALGEBRA

The mth order Hankel transform of a function f is defined as

$$\mathfrak{F}_m[f(r)] \equiv \mathfrak{f}_m(k_\perp) = \int_0^\infty dr\, r J_m(k_\perp r) f(r), \qquad (A1)$$

and, for reasonably well-behaved functions, the inversion theorem

$$f(r) = \int_0^\infty dk_\perp\, k_\perp J_m(k_\perp r)\, \mathfrak{f}_m(k_\perp), \qquad (A2)$$

applies. We now establish the algebra of these transforms when applied to the standard radial operators.

From the recurrence relation $(2m/x)J_m = J_{m-1} + J_{m+1}$, it follows immediately that

$$\mathfrak{F}_m\left[\frac{1}{r}f\right] = \frac{k_\perp}{2m}[\mathfrak{F}_{m-1}[f] + \mathfrak{F}_{m+1}[f]]. \qquad (A3)$$

While using $2J'_m = J_{m-1} - J_{m+1}$ and integrating by parts, we find

$$\mathfrak{F}_m\left[\frac{1}{r}\frac{\partial}{\partial r}rf\right] = \frac{k_\perp}{2}[\mathfrak{F}_{m+1}[f] - \mathfrak{F}_{m-1}[f]]. \qquad (A4)$$

In a similar manner, the following identities may be proved:

$$\mathfrak{F}_m\left[\frac{\partial}{\partial r}f\right] = \frac{k_\perp}{2m}[(m-1)\mathfrak{F}_{m+1}[f] - (m+1)\mathfrak{F}_{m-1}[f]], \qquad (A5)$$

$$\mathfrak{F}_m\left[\frac{1}{r^2}f\right] = \frac{k_\perp^2}{4}\left[\frac{1}{m(m-1)}\mathfrak{F}_{m-2}[f] + \frac{2}{m^2-1}\mathfrak{F}_m[f] + \frac{1}{m(m+1)}\mathfrak{F}_{m+2}[f]\right], \qquad (A6)$$

$$\mathfrak{F}_m\left[\frac{1}{r}\frac{\partial}{\partial r}r\frac{\partial}{\partial r}f\right] = \frac{k_\perp^2}{4}\left[\frac{m}{m+1}\mathfrak{F}_{m+2}[f] - \frac{2(m^2-2)}{m^2-1}\mathfrak{F}_m[f] + \frac{m}{m-1}\mathfrak{F}_{m-2}[f]\right]. \qquad (A7)$$

Equations (A6) and (A7) imply the familiar relation

$$\mathfrak{F}_m\left[\frac{1}{r}\frac{\partial}{\partial r}r\frac{\partial}{\partial r}f - \frac{m^2}{r^2}f\right] = -k_\perp^2\mathfrak{F}_m[f]. \qquad (A8)$$

It is straightforward, using these identities, to transform $\nabla\times\nabla\times\mathbf{A}$ (in cylindrical coordinates) into an algebraic system of equations. However, in general, this system is not closed with respect to the transforms; that is, mth order transforms are coupled to $m\pm1$, $m\pm2$ order transforms, and no simple relation between the different order transforms exists. For the special (azimuthally symmetric) case considered in this paper it was possible to choose the transforms such that the system remained closed. The resulting algebraic equations for the transforms were then formally identical to those for a artesian, slab, geometry. All cylindrical effects were absorbed by the transform kernel.

The advantage of such a technique for non-azimuthally symmetric waves is obvious. Some combination of the transforms may allow this. We have not, however, been able to demonstrate this for the general case.

[1] N. Rostoker, Bull. Am. Phys. Soc. **14**, 49 (1969); and G. B. Lubkin, Physics Today **22**, 59 (June, 1969).

[2] Y. B. Fainberg, V. D. Shapiro, and V. I. Shevchenko, Zh. Eksp. Teor. Fiz. **57**, 966 (1969) [Sov. Phys.-JETP **30**, 528 (1970)]; R. I. Kovtun and A. A. Rukhadze, Zh. Eksp. Teor. Fiz. **58**, 1709 (1970) [Sov. Phys.-JETP **31**, 915 (1970)]; L. E. Thode and R. N. Sudan, Phys. Rev. Lett. **30**, 732 (1973); R. V. Lovelance and R. N. Sudan, Phys. Rev. Lett. **27**, 1256 (1971).

[3] D. A. Hammer and N. Rostoker, Phys. Fluids **11**, 1831 (1970).

[4] C. A. Kapetanakos, W. M. Black, and K. R. Chu, Phys. Rev. Lett. **34**, 1156 (1975).

[5]K. R. Chu and N. Rostoker, Phys. Fluids **17**, 813 (1974).
[6]S. I. Braginskii, in *Reviews of Plasma Physics* (Consultants Bureau, New York, 1965), Vol. 1, p. 205.
[7]M. N. Rosenbluth and A. N. Kaufman, Phys. Rev. **109**, 1 (1958).
[8]K. R. Chu, C. A. Kapetanakos, and R. W. Clark, Appl. Phys. Lett. **27**, 185 (1975).
[9]R. Z. Sagdeev, in *Magneto-Fluid and Plasma Dynamics*, edited by H. Grad (American Mathematical Society, Providence, R.I., 1967), p. 281.
[10]D. Prono, B. Ecker, N. Bergstrom, and J. Benford, Phys. Rev. Lett. **35**, 438 (1975).
[11]L. E. Thode and R. N. Sudan, Phys. Fluids **18**, 1552 (1975); **18**, 1564 (1975).
[12]P. A. Miller and G. N. Kuswa, Phys. Rev. Lett. **30**, 958 (1973).
[13]G. C. Goldenbaum, W. F. Dove, K. A. Gerber, and B. G. Logan, Phys. Rev. Lett. **32**, 830 (1974).
[14]N. C. Christofilos, University of California Radiation Laboratory Reports 887 and 5617-T (1959).